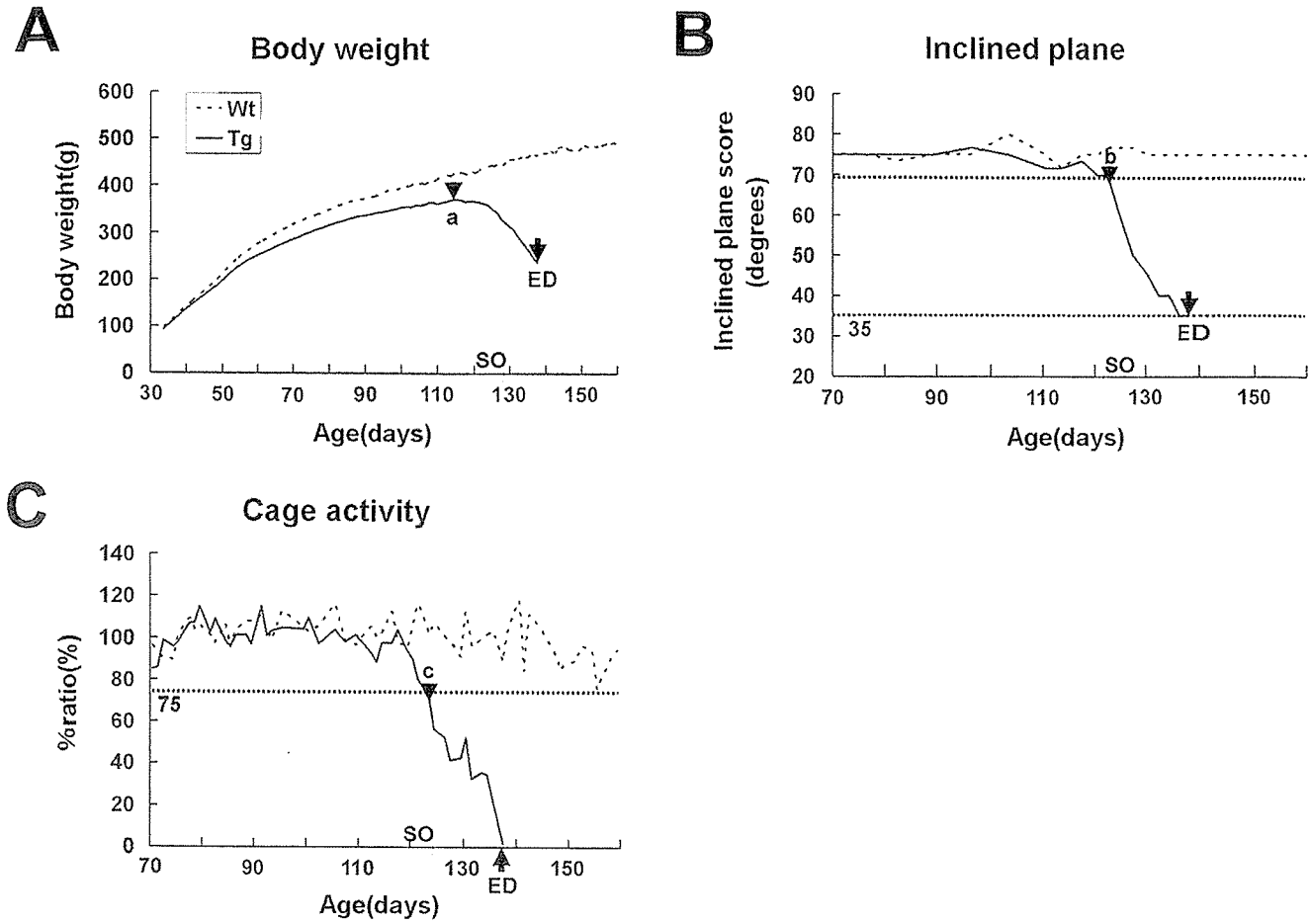

Fig. 4. Schematic presentation of the results from the body weight (**A**), inclined plane test (**B**), and cage activity (**C**) assessments. The onset defined by each measure (black arrowheads) and the end-stage of the disease (ED, black arrows) are indicated in the figures. a, pre-symptomatic onset: the day the transgenic rats scored their maximum body weight. b, muscle weakness onset: the earliest day the transgenic rats scored <70° in the inclined plane test. c, hypo-activity onset: the earliest day the transgenic rats scored <75% of the mean movements from 70–90 days of age in the cage activity measure. SO, subjective onset: the earliest day that observable functional deficits such as paralysis of the limbs or symptoms of general muscle weakness were observed subjectively in the open field (the gray shaded region in A–C).

60 days of age for all parameters (M1, M2, RG), however, even after the wild-type animals showed the decrease in their movement scores. The differences between the two groups increased markedly after 90 days of age for M1, M2, and RG (Fig. 3D–F). The performance of each rat fluctuated so markedly that the SCANET test seems to be inappropriate for statistical analysis.

Onset, End-Stage, and Duration of Disease in hSOD1 (G93A) Transgenic Rats

Using the quantitative analysis of disease progression by body-weight measurement, the inclined plane test, and cage activity, as described above, we defined three time points of "objective onset," as shown in Figure 4. The SCANET results did not allow us to define a time of objective onset, because we could not establish a stable baseline level using the data from the highly variable measurements we obtained, even for wild-type rats. The righting reflex failure was useful for detecting the time point of end-stage disease, which we defined as the generalized loss of motor activity in affected rats. A total of 20 transgenic rats assessed by body weight and the inclined plane test were analyzed for the day of objective onset, end-stage, and duration of the disease. The cage activity data from the eight transgenic rats were obtained simultaneously. The results are shown in Table IV.

The day the transgenic rats reached their maximum body weight was defined as pre-symptomatic onset (113.6 ± 4.8 days of age, black arrowhead in Fig. 4A, Table IV). This onset was judged retrospectively and always preceded the subjective onset (gray shaded region, Fig. 4A), which was determined by observable functional deficits in the open field, such as paralysis of limbs and symptoms of general muscle weakness. The

TABLE IV. Onset, End-Stage, and Duration in Days of Disease in hSOD1 (G93A) Transgenic Rats

Evaluation methods	Body weight and inclined plane (n = 20)	Cage activity (n = 8)
Objective onset		
Pre-symptomatic onset[a]	113.6 ± 4.8 (103–124)	
Muscle weakness onset[b]	125.2 ± 7.4 (110–144)	
Hypo-activity onset[c]		122.8 ± 9.2 (109–139)[c]
Subjective onset (SO)[d]	126.5 ± 7.1 (113–147)	121.3 ± 9.8 (109–140)
End-stage disease (ED)[e]	137.8 ± 7.1 (128–155)	134.1 ± 8.2 (122–149)
Duration[f]		
ED-a[g]	24.3 ± 6.5	
ED-b[h]	12.6 ± 3.5	
ED-c[i]		11.4 ± 1.3

Values are means ± SD.
[a] Maximum of body weight.
[b] Less than 70 degrees in the inclined plane test.
[c] Less than 75% in the mean movements of 70-90 days in the cage activity.
[d] Observable functional deficits.
[e] Righting reflex failure.
[f] Difference in days between ED and each onset;
[g] between ED and pre-symptomatic onset,
[h] between ED and muscle weakness onset,
[i] between ED and hypo-activity onset.

TABLE V. Comparison of the Onset, End-stage, and Duration in Days of Disease in the Forelimb-type and the Hindlimb-type Rats

	Forelimb type (n = 4)	Hindlimb type (n = 14)	General type* (n = 2)
Pre-symptomatic onset[a]	112.5 ± 6.7	114.6 ± 4.3	(108.5)
Muscle weakness onset[b]	125.8 ± 2.8	126.7 ± 7.3	(113.5)
End-stage disease (ED)[c]	134.0 ± 2.4	140.1 ± 7.1	(129.5)
Duration[d]			
ED-a[e]	21.5 ± 8.5	25.5 ± 6.2	(21)
ED-b[f]	8.3 ± 1.0	13.4 ± 3.0	(16)

Values are mean ± SD.
* Values of general-type rats are listed in parenthesis for reference.
[a] Maximum of body weight.
[b] Less than 70 degrees in the inclined plane test.
[c] Righting reflex failure.
[d] Difference in days between ED and each onset;
[e] between ED and pre-symptomatic onset,
[f] between ED and muscle weakness onset.

pre-symptomatic onset was the most sensitive of all the onset measures described in this study (Table IV).

The first day the transgenic rats scored <70° in the inclined plane test was defined as the muscle weakness onset (black arrowhead, Fig. 4B). We could judge this onset prospectively. Muscle weakness onset (125.2 ± 7.4 days of age, Table IV) was usually recorded before or at almost the same time as the subjective onset (8 days before to 1 day after, gray shaded region, Fig. 4B and 126.5 ± 7.1 days of age, Table IV). The day the transgenic rats scored 35° or less on the inclined plane test coincided with the day of righting reflex failure (black arrow, Fig. 4B).

The first day the transgenic rats scored <75% of their baseline movements in the cage activity test was defined as hypo-activity onset (black arrowhead, Fig. 4C and 122.8 ± 9.2 days of age, Table IV). We could also judge this onset prospectively. Hypo-activity onset was recorded 1 day before to 4 days after the subjective onset (SO, shown as the gray shaded region in Fig. 4C and 121.3 ± 9.8 days of age, Table IV). A 0% movement score for cage activity was seen at almost the same time as righting reflex failure (black arrow, Fig. 4C). Although disease onset and end-stage could be objectively defined with these methods, they had a wide range, of about 1 month, because of the diversity of the phenotypes (Table IV).

Differences in Disease Courses Between the Forelimb- and Hindlimb-Type Rats

Because we noticed variability in disease courses among different clinical types of hSOD1 (G93A) rats, we next assessed disease progression in 20 transgenic rats with forelimb- (n = 4), hindlimb- (n = 14), and general- (n = 2) type, using the probability of objective

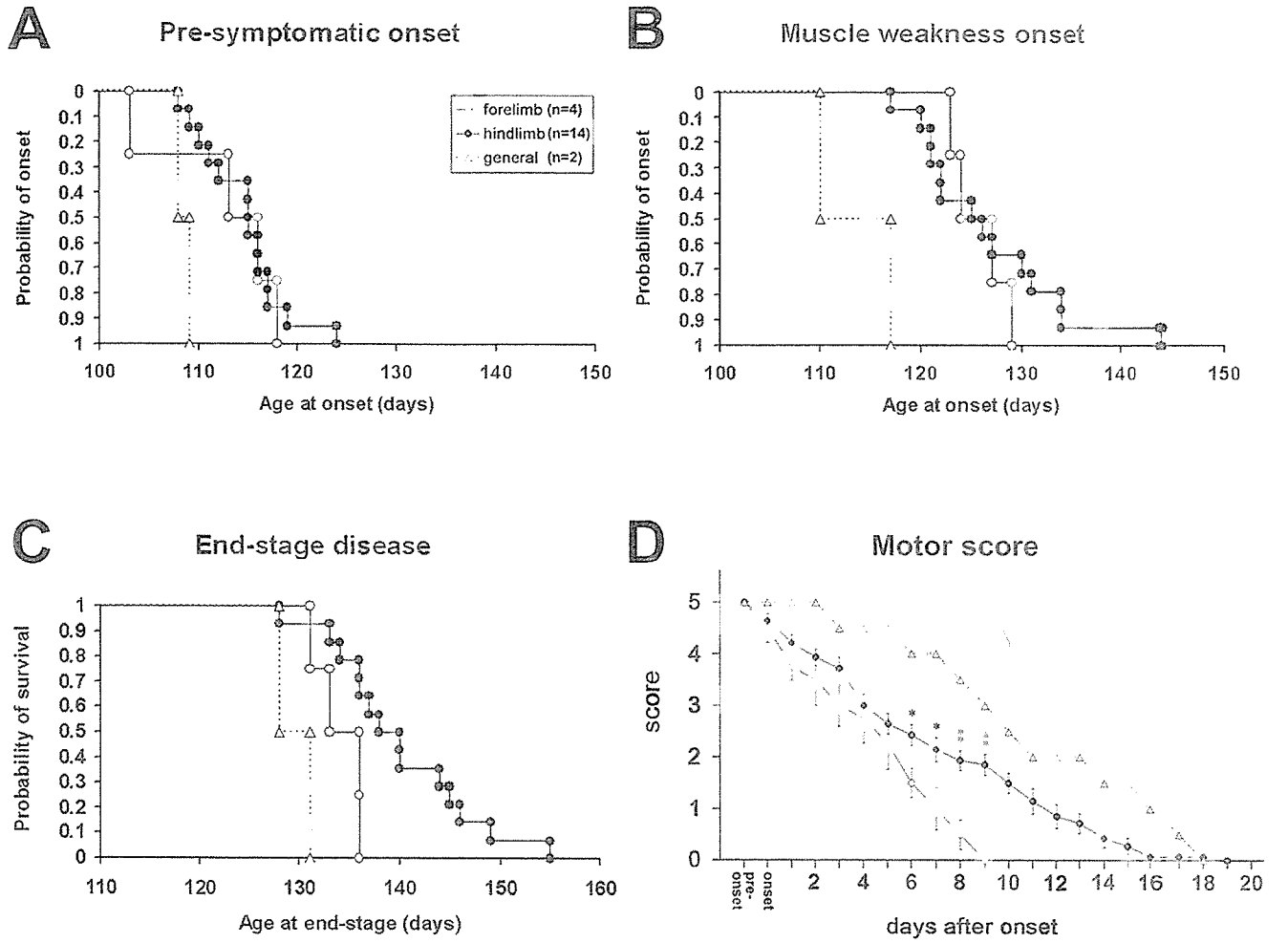

Fig. 5. Comparison of onset, end-stage, and disease progression in the forelimb-type ($n = 4$), and the hindlimb-type ($n = 14$) rats. Data from the general-type rats are also shown as dotted lines. **A,B:** The probability of the objective onsets. We did not see any differences in the probability of the objective onsets defined by body weight measurement (pre-symptomatic onset) and the inclined plane test (muscle weakness onset) between the forelimb- and hindlimb-type rats. **C:** The probability of survival as defined by end-stage disease. Survival was significantly shorter in the forelimb-type than in the hindlimb-type rats ($P < 0.05$, Log-rank test). **D:** Assessment of disease progression using the Motor score. Affected rats were evaluated after muscle weakness onset. The forelimb type worsened more quickly than the hindlimb type. Score decline correlated well with the exacerbation of symptoms in both clinical types, clearly and objectively. Bars = means ± SEM. Statistically significant differences between forelimb and hindlimb types are indicated in the figures. $^{*}P < 0.05$. $^{**}P < 0.01$; two-tailed unpaired Student's t-test.

onsets (pre-symptomatic onset and muscle weakness onset), the probability of survival defined by end-stage disease (failure in righting reflex), and the Motor score (Table V, Fig. 5). We did not see any differences in the objective onsets between the forelimb- and hindlimb-type rats (Fig. 5AB, Table V). However, survival as defined by end-stage disease was significantly shorter in the forelimb-type than in the hindlimb-type rats ($P < 0.05$, Log-rank test, Fig. 5C). Moreover, the duration of the disease calculated from the muscle weakness onset was also significantly shorter in the forelimb-type (8.3 ± 1.0 days) than in the hindlimb-type rats (13.4 ± 3.0 days) (see ED – b, $P < 0.01$, two-tailed unpaired Student's t-test, Table V).

The courses of functional deterioration evaluated by the Motor score after onset (muscle weakness onset) for each clinical type were well represented by the declines in their scores (Fig. 5D). The assessment by the Motor score also showed that disease progression in the forelimb type was more rapid than that in the hindlimb type (Fig. 5D).

Our results raise the question of why this variability in the disease course of each clinical type was observed. We speculated that there might be correlation between clinical type in G93A rats and the amount of locally expressed mutant hSOD1 (G93A) gene product. Therefore, we next investigated expression of the mutant hSOD1 gene in each segment of the spinal cord (cervical, thoracic, and lumbar) in the forelimb- and

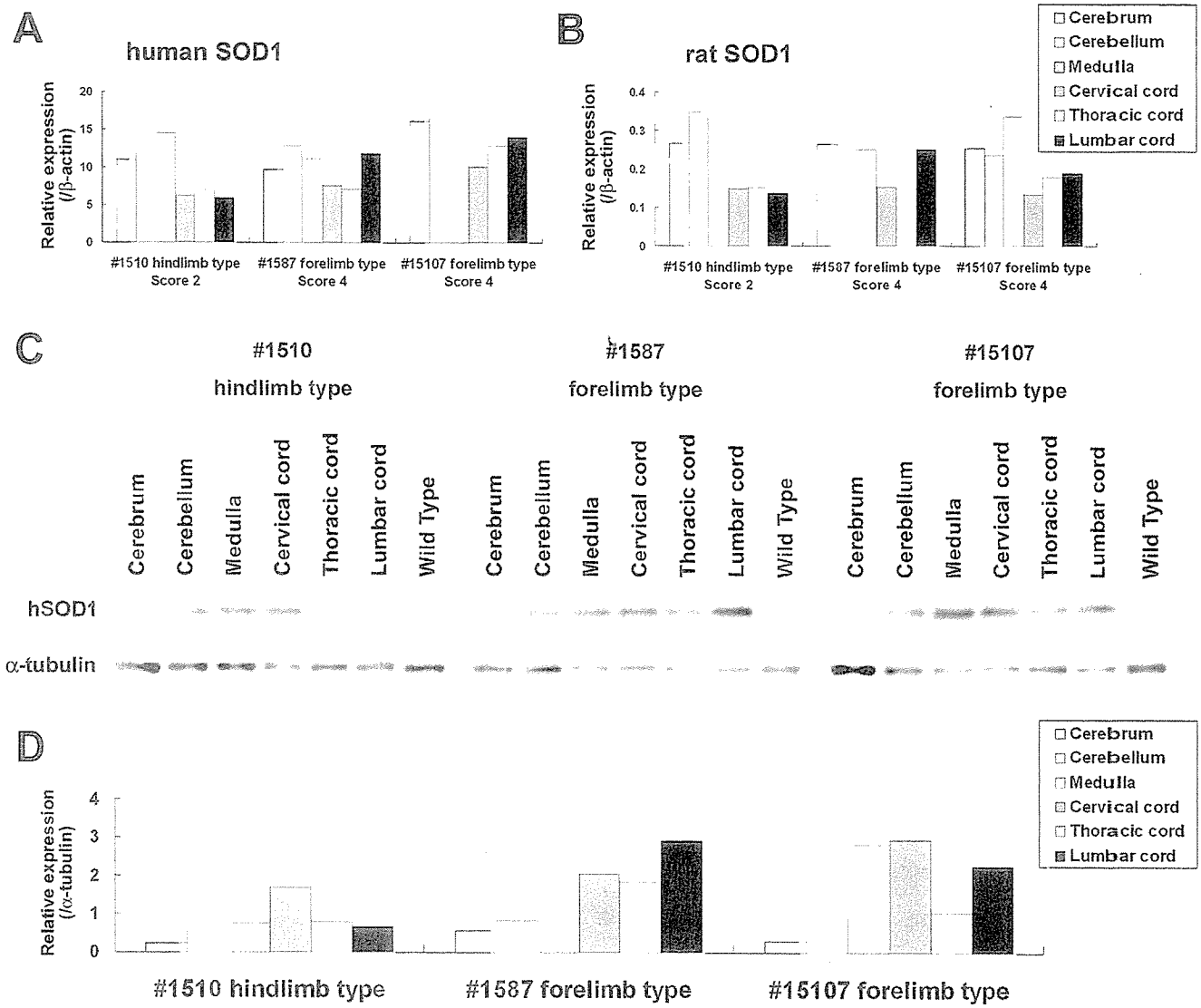

Fig. 6. The expression of mutant hSOD1 mRNA and protein in the cerebral cortex, cerebellum, medulla, and spinal cord (cervical, thoracic, and lumbar) of forelimb- and hindlimb-type rats. **A,B:** The amounts of human (A) and endogenous rat (B) SOD1 mRNA normalized to those of *β-actin* were quantified by real time RT-PCR analysis. **C,D:** Western blot analysis of the mutant hSOD1 protein was carried out in the same rats. Quantitative analysis was carried out with a Scion Image. The amounts of proteins were normalized to those of α-tubulin (D).

hindlimb-type rats by real time RT-PCR and Western blot analysis. However, at least at the stages after the apparent onset of muscle weakness, neither forelimb-type (#1587, Score 4 and #15107, Score 4) nor hindlimb-type rats (#1510, Score 2) necessarily expressed larger amounts of the mutant hSOD1 (G93A) transgene in the cervical cord or in the lumbar cord, respectively, at the mRNA and the protein level (Fig. 6). We also investigated the expression of endogenous rat SOD1 mRNA in the same rats by REAL TIME RT-PCR (Fig. 6B). Distribution of endogenous rat SOD1 mRNA expressed in each segment of the spinal cord showed almost the same pattern as that of mutant hSOD1 mRNA. The expression of endogenous rat SOD1 mRNA was lower than that of mutant hSOD1 mRNA. Thus, we could not detect any definite correlation between the hSOD1 (G93A) transgene local expression profile in the spinal cord and the phenotypes of G93A rats for either the forelimb-type or the hindlimb-type rats (Fig. 6).

Reduction in the Number of Spinal Cord Motor Neurons at Different Disease Stages

We examined histo-pathological changes in the spinal cords of the transgenic rats in comparison with those

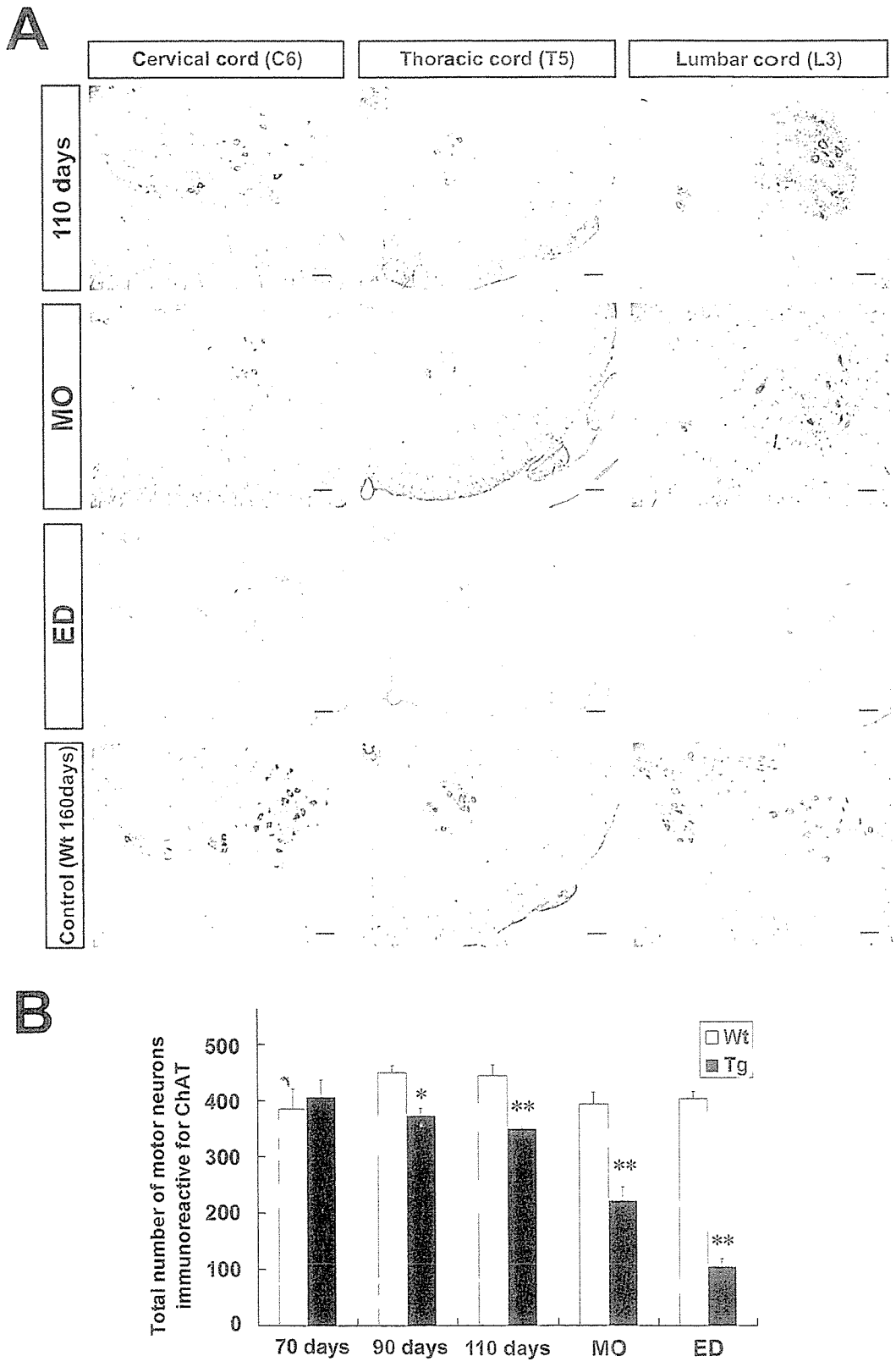

Fig. 7. The loss of motor neurons in the spinal cord of hSOD1 (G93A) transgenic rats at different stages. **A:** Immunohistochemical analysis of the spinal cord of transgenic rats. Transverse sections of the cervical (C6), thoracic (T5), and lumbar (L3) spinal cord of the transgenic rats and their wild-type littermates were stained with an anti-ChAT antibody to label viable motor neurons at the indicated stages (Scale bars = 100 μm). **B:** The number of ChAT immunoreactive motor neurons was counted and is shown in the histograms as the total number of motor neurons in the C6, T5, and L3 segments. This number began to decrease in the transgenic rats at 90 days of age, rapidly declined after 110 days of age, and fell to about 50% and 25% of wild-type rats at the muscle weakness onset (MO, around 125 days) and at end-stage disease (ED, around 140 days), respectively. Bars = means ± SEM ($n = 3$ for each genotype). $^{*}P < 0.05$. $^{**}P < 0.01$; two-tailed unpaired Student's t-test.

of their wild-type littermates at 70, 90, and 110 days of age, when the transgenic rats scored <70° in the inclined plane test (muscle weakness onset), and failed the righting reflex. To quantify the number of spinal motor neurons, we stained spinal cord sections of both groups with an anti-ChAT antibody.

As shown in Figure 7A, the numbers of ChAT immunoreactive motor neurons in the cervical (C6), thoracic (T5), and lumbar (L3) segments of the spinal cord decreased with disease progression. Quantitative analysis of the residual motor neurons showed that the total number of motor neurons in the transgenic rats began to decrease at 90 days of age, rapidly declined after 110 days of age, and fell to about 50% and 25% of the numbers in age-matched wild-type littermates at the time the score was <70° in the inclined plane test (muscle weakness onset) and of righting reflex failure, respectively (Fig. 7B).

TABLE VI. Adequacy of Evaluation Methods in Regard to Practical Use*

	Body weight	Inclined plane	Cage activity	SCANET	Motor score
Objectivity	A	B	A	A	B
Sensitivity	A	B	C	(A)	-
Specificity	C	B	C	C	A
Motivation independence	A	B	B	D	B
Skill requirements	A	B	A	A	B
Cost of apparatus	B	B	D	D	A

*A, more appropriate; B, appropriate; C, less appropriate; D, inappropriate.

DISCUSSION

Factors Underlying the Variability in Phenotypes of hSOD1 (G93A) Transgenic Rats

In previous studies of this G93A rat, only the hindlimb-type has been described, and the variety of phenotypes and variable clinical courses have not yet been mentioned (Nagai et al., 2001). Recently, however, another line of G93A rats backcrossed onto a Wistar background ($SOD1^{G93A/HWr}$ rats) was reported to present two phenotypes, including forelimb-type, and a large inter-litter variability in disease onset (Storkebaum et al., 2005). In the same way, commonly used FALS model mice harboring hSOD1 (G93A) gene have been reported to have clinical variability to some extent, and some of them dominantly show forelimb paralysis (Gurney et al., 1994). In this study, we recognized various clinical types, including forelimb-, hindlimb-, and general-type and established quantitative methods to evaluate disease progression that can be applied to any of the clinical types of this ALS model. We have also shown the variability in disease progression to depend on clinical types, that is, disease progression after the onset was faster in forelimb-type than in hindlimb-type rats. This difference may be due to the aggressiveness of the disease per se because we evaluated the time point of "death" (end-stage disease) according to righting reflex failure (Howland et al., 2002) to exclude the influence of feeding problems (bulbar region) and respiratory failure (level C2–C4).

These findings give rise to the next question; why is this variety of phenotypes and variability in the clinical course observed in the same transgenic line? There are at least three possible explanations. One is that the variation is due to the heterogeneous genetic background of the Sprague-Dawley (SD) rat (i.e., the strain used to generate this transgenic line), which might have led to different phenotypes. This idea is supported by the fact that the SD strain shows a large inter-individual disease variability in other models of neurodegenerative disorders, such as Huntington's disease (Ouary et al., 2000). Similar phenotypic variability takes place in human FALS carrying the same mutations in hSOD1 gene (Abe et al., 1996; Watanabe et al., 1997; Kato et al., 2001), which could be explained by heterogeneous genetic backgrounds. Thus, the present transgenic ALS model rats may be highly useful to understand the mechanisms of bulbar onset, arm onset, or leg onset that are seen in human disease. There may be modifier genes of these phenotypes, which should be identified in the future study.

The second is that there is variability in the expression of the mutant hSOD1 protein. The transcriptional regulation of this exogenous gene could be affected by one or more unknown factors, such as epigenetic regulation, and may not be expressed uniformly throughout the spinal cord of each animal. Therefore, some rats might express mutant proteins more in the cervical spinal cord and others might express more in the lumber cord, possibly resulting in the forelimb type and hindlimb type, respectively. However, we found no definite correlation between local expression levels of the mutant hSOD1 mRNA/protein in the spinal cord and the phenotypes of these animals, using real time RT-PCR and western blot analysis after the onset of muscle weakness, when the clinical type of the transgenic rats could be defined (Fig. 6). Moreover, the pathological analysis showed no correlation between the number of residual motor neurons in each segment and the phenotypes of end-stage animals. However, because >50% of spinal motor neurons have already degenerated at the stage of muscle weakness onset, whether local expression of the mutant hSOD1 gene and segmental loss of motor neurons correlate with the clinical types of G93A rats should be further investigated by analyzing younger animals at a stage when motor neuron loss has not progressed as much.

The third explanation involves a structural property of the mutant hSOD1 (G93A) protein itself. It is now thought that mutations in the hSOD1 gene may alter the 3-D conformation of the enzyme and, in turn, result in the SOD1 protein acquiring toxic properties that cause ALS (Deng et al., 1993; Hand and Rouleau 2002). For instance, the hSOD1 (G93A) mutant protein has been reported to be susceptible to nonnative protein–protein interactions because of its mutation site and unfolded structure (Shipp et al., 2003; Furukawa and

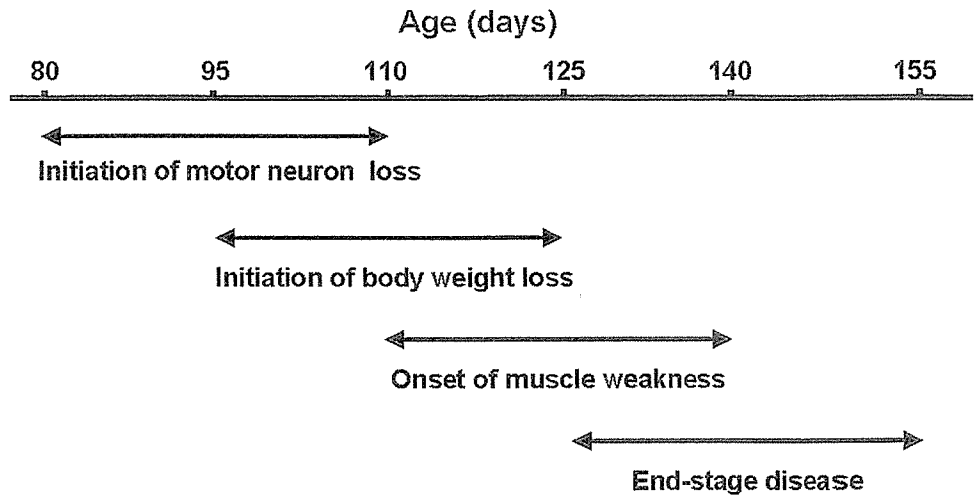

Fig. 8. Four stages of disease progression in hSOD1 (G93A) transgenic rats. The disease progression can be classified into four stages as shown. The range for each stage is about 1 month and overlaps approximately 2 weeks with the next stage.

O'Halloran, 2005), suggesting that the G93A mutation might accelerate the formation of SOD1 protein aggregates, which may ultimately sequester heat-shock proteins and molecular chaperones, disturb axonal transport or protein degradation machineries, including the ubiquitin-proteasome system (Borchelt et al., 1998; Bruening et al., 1999; Williamson and Cleveland 1999; Okado-Matsumoto and Fridovich 2002; Urushitani et al., 2002). Curiously, the mutated hSOD1 (G93A) protein is more susceptible to degradation by the ubiquitin-proteasome system and has a shorter half-life than other mutants (Fujiwara et al., 2005), suggesting that it may cause more unstable toxic aggregates in the spinal cord than other mutations. The degradation rate is also affected by environmental factors unique to each animal, such as the progressive decline of proteasome function with age (Keller et al., 2000), and these factors could contribute to the variability of the clinical course of G93A rats.

Taking all these findings into consideration, the mutated hSOD1 (G93A) protein may gain properties that are responsible for a variety of phenotypes and variability in the clinical course of the affected animals.

Characteristics of Different Methods for Assessing hSOD1 (G93A) Transgenic Rats

The ideal measure is not influenced by the judgment of the observer, sensitive to small abnormalities, specific to detect pathologic events that are related to pathogenesis of the ALS-like disease, not influenced by the motivational factors of rats, minimal in the requirements for skill in the observer, and inexpensive to carry out. We assessed each evaluation method by the categories in regard to practical use as shown in the Table 6.

The initiation of body weight loss seems to be an excellent marker to detect the onset and should be highly recommended. Muscle volume might have already started to decrease, even in the period of continuous weight gain, as reported for hSOD1 (G93A) transgenic mice (Brooks et al., 2004). As a result, it could detect an abnormality relatively earlier than subjective onset. The inclined plane test is considered to be the least defective method of all. It could objectively and specifically detect the decline in the muscle strength of these ALS model rats as a muscle weakness onset almost at the same time of the subjective onset. The cage activity measurement and SCANET require very expensive apparatus, and are limited by the availability of funds and space for making the measurements. Although SCANET test was most sensitive among these measures, it seems inappropriate for the statistical analysis, and does not add any more information than that obtained through simple observation of the rats because the performances of the rats might be severely affected by the extent of their motivation to explore. Motor score can specifically assess disease progression of each clinical type and is valuable in keeping the experimental costs at a minimum.

Correlation Between the Loss of Spinal Motor Neurons and Disease Stages

This study clearly shows the variable clinical course of G93A rats. According to our behavioral and histological analyses, we can divide the disease course of this transgenic model into four stages, whose durations have a range of about 1 month, as shown in Figure 8. Furthermore, we have established the pathological validity of the performance deficits detected by each measure of disease progression. "Initiation of motor neuron loss" was defined as a statistically significant decrease in the number of spinal motor neurons, which was found at around 90 days of age, but not 70 days of age (Fig. 7B). This coincides with, and seems to be sensitively detected by the marked difference in SCANET scores that begins at around 90 days of age (Fig. 3D–F). The "initiation of body weight loss" was usually detected at around 110 days of age as the peak body weight (pre-symptomatic onset, 113.6 ± 4.8 days of age, range = 103–124, Table IV). This stage coincides with the initiation of a rapid decline in the number of motor neurons at around 110 days of age (Fig. 7B). "Onset of muscle weakness" was detected at around 125 days of age, as assessed by the

inclined plane test (muscle weakness onset, 125.2 ± 7.4 days of age, range = 110–144, Table IV). This coincides with the number of spinal motor neurons in the transgenic rats being reduced to about 50% of the number in wild-type rats (Fig. 7B). We presume that transgenic rats do not present obvious muscle weakness until the number of motor neurons has been reduced to approximately half the number found in the healthy state. "End-stage disease" as defined by righting reflex failure was recorded at around 140 days of age (137.8 ± 7.1 days of age, range = 122–155, Table IV). At this stage, the affected rats had only about 25% of the spinal motor neurons of age- and gender-matched wild-type rats (Fig. 7B), and showed a generalized loss of motor activity. Thus, our findings allow us to estimate the extent of spinal motor neuron loss by evaluating the disease stage with the measures described in this study.

In summary, we have described the variable phenotypes of mutant hSOD1 (G93A) transgenic rats and established an evaluation system applicable to all clinical types of these rats. Disease stages defined by this evaluation system correlated well pathologically with the reduction of motor neurons. Our evaluation system of this animal model should be a valuable tool for future preclinical experiments aimed at developing novel treatments for ALS.

ACKNOWLEDGMENTS

We thank Dr. H.-N. Dai of the Department of Neuroscience, Georgetown University School of Medicine for technical advice and valuable discussions, and Dr. T. Yoshizaki and Miss K. Kaneko for participating in the assessment of transgenic rats with the Motor score. This work was supported by grants from CREST, Japan Society for the Promotion of Science to H.O., a Research Grant on Measures for Intractable Diseases from the Japanese Ministry of Health, Labour and Welfare to H.O., M.A., G.S. and Y.I., and a Grant-in-Aid for the 21st century COE program to Keio University from the Japanese Ministry of Education, Culture, Sports, Science and Technology.

REFERENCES

Abe K, Aoki M, Ikeda M, Watanabe M, Hirai S, Itoyama Y. 1996. Clinical characteristics of familial amyotrophic lateral sclerosis with Cu/Zn superoxide dismutase gene mutations. J Neurol Sci 136:108–116.

Azzouz M, Ralph GS, Storkebaum E, Walmsley LE, Mitrophanous KA, Kingsman SM, Carmeliet P, Mazarakis ND. 2004. VEGF delivery with retrogradely transported lentivector prolongs survival in a mouse ALS model. Nature 429:413–417.

Barneoud P, Lolivier J, Sanger DJ, Scatton B, Moser P. 1997. Quantitative motor assessment in FALS mice: a longitudinal study. Neuroreport 8:2861–2865.

Borchelt DR, Wong PC, Becher MW, Pardo CA, Lee MK, Xu ZS, Thinakaran G, Jenkins NA, Copeland NG, Sisodia SS, Cleveland DW, Price DL, Hoffman PN. 1998. Axonal transport of mutant superoxide dismutase 1 and focal axonal abnormalities in the proximal axons of transgenic mice. Neurobiol Dis 5:27–35.

Brooks KJ, Hill MD, Hockings PD, Reid DG. 2004. MRI detects early hindlimb muscle atrophy in Gly93Ala superoxide dismutase-1 (G93A SOD1) transgenic mice, an animal model of familial amyotrophic lateral sclerosis. NMR Biomed 17:28–32.

Brown RH Jr. 1995. Amyotrophic lateral sclerosis: recent insights from genetics and transgenic mice. Cell 80:687–692.

Bruening W, Roy J, Giasson B, Figlewicz DA, Mushynski WE, Durham HD. 1999. Up-regulation of protein chaperones preserves viability of cells expressing toxic Cu/Zn-superoxide dismutase mutants associated with amyotrophic lateral sclerosis. J Neurochem 72:693–699.

Chiu AY, Zhai P, Dal Canto MC, Peters TM, Kwon YW, Prattis SM, Gurney ME. 1995. Age-dependent penetrance of disease in a transgenic mouse model of familial amyotrophic lateral sclerosis. Mol Cell Neurosci 6:349–362.

de Belleroche J, Orrell R, King A. 1995. Familial amyotrophic lateral sclerosis/motor neurone disease (FALS): a review of current developments. J Med Genet 32:841–847.

Deng HX, Hentati A, Tainer JA, Iqbal Z, Cayabyab A, Hung WY, Getzoff ED, Hu P, Herzfeldt B, Roos RP, Warner C, Deng G, Soriano E, Smyth C, Parge HE, Ahmed A, Roses AD, Hallewell RA, Pericak-Vance MA, Siddique T. 1993. Amyotrophic lateral sclerosis and structural defects in Cu, Zn superoxide dismutase. Science 261:1047–1051.

Fujiwara N, Miyamoto Y, Ogasahara K, Takahashi M, Ikegami T, Takamiya R, Suzuki K, Taniguchi N. 2005. Different immunoreactivity against monoclonal antibodies between wild-type and mutant copper/zinc superoxide dismutase linked to amyotrophic lateral sclerosis. J Biol Chem 280:5061–5070.

Furukawa Y, O'Halloran TV. 2005. Amyotrophic lateral sclerosis mutations have the greatest destabilizing effect on the Apo- and reduced form of SOD1, leading to unfolding and oxidative aggregation. J Biol Chem 280:17266–17274.

Gale K, Kerasidis H, Wrathall JR. 1985. Spinal cord contusion in the rat: behavioral analysis of functional neurologic impairment. Exp Neurol 88:123–134.

Garbuzova-Davis S, Willing AE, Milliken M, Saporta S, Zigova T, Cahill DW, Sanberg PR. 2002. Positive effect of transplantation of hNT neurons (NTera 2/D1 cell-line) in a model of familial amyotrophic lateral sclerosis. Exp Neurol 174:169–180.

Gurney ME, Pu H, Chiu AY, Dal Canto MC, Polchow CY, Alexander DD, Caliendo J, Hentati A, Kwon YW, Deng HX, Chen W, Zhai F, Sufit RL, Siddique T. 1994. Motor neuron degeneration in mice that express a human Cu,Zn superoxide dismutase mutation. Science 264:1772–1775.

Hand CK, Rouleau GA. 2002. Familial amyotrophic lateral sclerosis. Muscle Nerve 25:135–159.

Howland DS, Liu J, She Y, Goad B, Maragakis NJ, Kim B, Erickson J, Kulik J, DeVito L, Psaltis G, DeGennaro LJ, Cleveland DW, Rothstein JD. 2002. Focal loss of the glutamate transporter EAAT2 in a transgenic rat model of SOD1 mutant-mediated amyotrophic lateral sclerosis (ALS). Proc Natl Acad Sci USA 99:1604–1609.

Inoue H, Tsukita K, Iwasato T, Suzuki Y, Tomioka M, Tateno M, Nagao M, Kawata A, Saido TC, Miura M, Misawa H, Itohara S, Takahashi R. 2003. The crucial role of caspase-9 in the disease progression of a transgenic ALS mouse model. EMBO J 22:6665–6674.

Kaspar BK, Llado J, Sherkat N, Rothstein JD, Gage FH. 2003. Retrograde viral delivery of IGF-1 prolongs survival in a mouse ALS model. Science 301:839–842.

Kato M, Aoki M, Ohta M, Nagai M, Ishizaki F, Nakamura S, Itoyama Y. 2001. Marked reduction of the Cu/Zn superoxide dismutase polypeptide in a case of familial amyotrophic lateral sclerosis with the homozygous mutation. Neurosci Lett 312:165–168.

Keller JN, Huang FF, Zhu H, Yu J, Ho YS, Kindy TS. 2000. Oxidative stress-associated impairment of proteasome activity during ischemia-reperfusion injury. J Cereb Blood Flow Metab 20:1467–1473.

Landis JR, Koch GG. 1977. The measurement of observer agreement for categorical data. Biometrics 33:159–174.

Mikami Y, Toda M, Watanabe M, Nakamura M, Toyama Y, Kawakami Y. 2002. A simple and reliable behavioral analysis of locomotor function after spinal cord injury in mice. Technical note. J Neurosurg Spine 97:142–147.

Mulder DW, Kurland LT, Offord KP, Beard CM. 1986. Familial adult motor neuron disease: amyotrophic lateral sclerosis. Neurology 36:511–517.

Nagai M, Aoki M, Miyoshi I, Kato M, Pasinelli P, Kasai N, Brown RH, Jr., Itoyama Y. 2001. Rats expressing human cytosolic copper-zinc superoxide dismutase transgenes with amyotrophic lateral sclerosis: associated mutations develop motor neuron disease. J Neurosci 21:9246–9254.

Ohki-Hamazaki H, Sakai Y, Kamata K, Ogura H, Okuyama S, Watase K, Yamada K, Wada K. 1999. Functional properties of two bombesin-like peptide receptors revealed by the analysis of mice lacking neuromedin B receptor. J Neurosci 19:948–954.

Okada Y, Shimazaki T, Sobue G, Okano H. 2004. Retinoic-acid-concentration-dependent acquisition of neural cell identity during in vitro differentiation of mouse embryonic stem cells. Dev Biol 275:124–142.

Okado-Matsumoto A, Fridovich I. 2002. Amyotrophic lateral sclerosis: a proposed mechanism. Proc Natl Acad Sci USA 99:9010–9014.

Ouary S, Bizat N, Altairac S, Menetrat H, Mittoux V, Conde F, Hantraye P, Brouillet E. 2000. Major strain differences in response to chronic systemic administration of the mitochondrial toxin 3-nitropropionic acid in rats: implications for neuroprotection studies. Neuroscience 97:521–530.

Rivlin AS, Tator CH. 1977. Objective clinical assessment of motor function after experimental spinal cord injury in the rat. J Neurosurg 47: 577–581.

Rosen DR, Siddique T, Patterson D, Figlewicz DA, Sapp P, Hentati A, Donaldson D, Goto J, O'Regan JP, Deng HX, Rahmani Z, Krizus A, McKenna-Yasek D, Cayabyab A, Gasten SM, Berger R, Tanzi RE, Halperin JJ, Herzfeldt B, van den Bergh R, Hung WY, Bird T, Deng G, Mulder DW, Smyth C, Laing NG, Soriano E, Pericak-Vance MA, Haines J, Reuleau GA, Gusella JS, Horvitz HR, Brown RH Jr. 1993. Mutations in Cu/Zn superoxide dismutase gene are associated with familial amyotrophic lateral sclerosis. Nature 362:59–62.

Shipp EL, Cantini F, Bertini I, Valentine JS, Banci L. 2003. Dynamic properties of the G93A mutant of copper-zinc superoxide dismutase as detected by NMR spectroscopy: implications for the pathology of familial amyotrophic lateral sclerosis. Biochemistry 42:1890–1899.

Storkebaum E, Lambrechts D, Dewerchin M, Moreno-Murciano MP, Appelmans S, Oh H, Van Damme P, Rutten B, Man WY, De Mol M, Wyns S, Manka D, Vermeulen K, Van Den Bosch L, Mertens N, Schmitz C, Robberecht W, Conway EM, Collen D, Moons L, Carmeliet P. 2005. Treatment of motoneuron degeneration by intracerebroventricular delivery of VEGF in a rat model of ALS. Nat Neurosci 8:85–92.

Sun W, Funakoshi H, Nakamura T. 2002. Overexpression of HGF retards disease progression and prolongs life span in a transgenic mouse model of ALS. J Neurosci 22:6537–6548.

Urushitani M, Kurisu J, Tsukita K, Takahashi R. 2002. Proteasomal inhibition by misfolded mutant superoxide dismutase 1 induces selective motor neuron death in familial amyotrophic lateral sclerosis. J Neurochem 83:1030–1042.

Wang LJ, Lu YY, Muramatsu S, Ikeguchi K, Fujimoto K, Okada T, Mizukami H, Matsushita T, Hanazono Y, Kume A, Nagatsu T, Ozawa K, Nakano I. 2002. Neuroprotective effects of glial cell line-derived neurotrophic factor mediated by an adeno-associated virus vector in a transgenic animal model of amyotrophic lateral sclerosis. J Neurosci 22: 6920–6928.

Watanabe M, Aoki M, Abe K, Shoji M, Iizuka T, Ikeda Y, Hirai S, Kurokawa K, Kato T, Sasaki H, Itoyama Y. 1997. A novel missense point mutation (S134N) of the Cu/Zn superoxide dismutase gene in a patient with familial motor neuron disease. Hum Mutat 9:69–71.

Weydt P, Hong SY, Kliot M, Moller T. 2003. Assessing disease onset and progression in the SOD1 mouse model of ALS. Neuroreport 14: 1051–1054.

Williamson TL, Cleveland DW. 1999. Slowing of axonal transport is a very early event in the toxicity of ALS-linked SOD1 mutants to motor neurons. Nat Neurosci 2:50–56.

Journal of Cerebral Blood Flow & Metabolism (2006) 26, 1176–1188

www.jcbfm.com

Novel therapeutic strategy for stroke in rats by bone marrow stromal cells and *ex vivo* HGF gene transfer with HSV-1 vector

Ming-Zhu Zhao[1,2], Naosuke Nonoguchi[1], Naokado Ikeda[1], Takuji Watanabe[1], Daisuke Furutama[3], Daisuke Miyazawa[4], Hiroshi Funakoshi[4], Yoshinaga Kajimoto[1], Toshikazu Nakamura[4], Mari Dezawa[5], Masa-Aki Shibata[6], Yoshinori Otsuki[6], Robert S Coffin[7], Wei-Dong Liu[2], Toshihiko Kuroiwa[1] and Shin-Ichi Miyatake[1]

[1]*Department of Neurosurgery, Osaka Medical College, Takatsuki, Osaka, Japan;* [2]*Department of Neurosurgery, Pu Nan Hospital, Shanghai, People's Republic of China;* [3]*First Department of Internal Medicine, Osaka Medical College, Takatsuki, Osaka, Japan;* [4]*Division of Molecular Regenerative Medicine, Osaka University Graduate School of Medicine, Suita, Osaka, Japan;* [5]*Department of Anatomy and Neurobiology, Kyoto University Graduate School of Medicine, Kyoto, Japan;* [6]*Department of Anatomy and Biology, Osaka Medical College, Takatsuki, Osaka, Japan;* [7]*Department of Molecular Pathology in Windeyer Institute of Medical Sciences of University College, London, UK*

Occlusive cerebrovascular disease leads to brain ischemia that causes neurological deficits. Here we introduce a new strategy combining mesenchymal stromal cells (MSCs) and *ex vivo* hepatocyte growth factor (HGF) gene transferring with a multimutated herpes simplex virus type-1 vector in a rat transient middle cerebral artery occlusion (MCAO) model. Gene-transferred MSCs were intracerebrally transplanted into the rats' ischemic brains at 2 h (superacute) or 24 h (acute) after MCAO. Behavioral tests showed significant improvement of neurological deficits in the HGF-transferred MSCs (MSC-HGF)-treated group compared with the phosphate-buffered saline (PBS)-treated and MSCs-only-treated group. The significant difference of infarction areas on day 3 was detected only between the MSC-HGF group and the PBS group with the superacute treatment, but was detected among each group on day 14 with both transplantations. After the superacute transplantation, we detected abundant expression of HGF protein in the ischemic brain of the MSC-HGF group compared with others on day 1 after treatment, and it was maintained for at least 2 weeks. Furthermore, we determined that the increased expression of HGF was derived from the transferred *HGF* gene in gene-modified MSCs. The percentage of apoptosis-positive cells in the ischemic boundary zone (IBZ) was significantly decreased, while that of remaining neurons in the cortex of the IBZ was significantly increased in the MSC-HGF group compared with others. The present study shows that combined therapy is more therapeutically efficient than MSC cell therapy alone, and it may extend the therapeutic time window from superacute to acute phase.
Journal of Cerebral Blood Flow & Metabolism (2006) **26,** 1176–1188. doi:10.1038/sj.jcbfm.9600273; published online 18 January 2006

Keywords: gene transfer; hepatocyte growth factor; herpes simplex virus; intracerebral transplantation; mesenchymal stromal cell; transient cerebral ischemia

Correspondence: Dr S-I Miyatake and Dr T Kuroiwa, Department of Neurosurgery, Graduate School of Medicine, Osaka Medical College, 2-7 Daigakumachi, Takatsuki City, Osaka 569-8686, Japan. E-mail: neu070@poh.osaka-med.ac.jp
This work was supported by Grants-in-Aid for Scientific Research (B) (14370448) and (C) (12671353), and by a Grant-in-Aid for Exploratory Research (14657350) from the Japanese Ministry of Education, Science and Culture, Japan to Shin-Ichi Miyatake, MD, PhD. Additional support was provided in the form of a grant from the Special Assistance for Promoting the Advancement of the Education & Research of the Private University, Promotion and Mutual Aid Corporation for Private Schools of Japan and the Science Research Promotion Fund to Shin-Ichi Miyatake, MD, PhD, and by the High-Tech Research Program of Osaka Medical College. This work was also supported in part by Grants-in-Aid 17790989 from the Ministry of Education, Science and Culture, Japan to Naosuke Nonoguchi, MD.
Received 22 August 2005; revised 29 November 2005; accepted 5 December 2005; published online 18 January 2006

Introduction

Occlusive cerebrovascular disease often causes global ischemia of the brain and results in neuropathological changes. Several methods have been proposed to augment brain reorganization, including the stimulation of endogenous processes through pharmacologic or molecular manipulation, gene therapy, behavioral and rehabilitation strategies, and the provision of new substrates for recovery through cell therapy.

Bone marrow contains the precursors of nonhematopoietic tissues that are referred to as mesenchymal stem cells or marrow stromal cells (MSCs) (Friedenstein *et al*, 1978). Marrow stromal cells are characterized by the ability to self-renew in a

number of nonhematopoietic tissues, and by their multipotentiality for differentiation into various tissues, such as fibroblasts, bone, muscle, and cartilage (Caplan and Bruder, 2001; Phinney, 2002). Additionally, they share some characteristics of neurons and astrocytes when cultured *in vitro* (Kim *et al*, 2002) or after being implanted into the central nervous system *in vivo* (Chopp *et al*, 2000; Nakano *et al*, 2001; Li *et al*, 2001, 2002; Chen *et al*, 2002*a*, *b*). Marrow stromal cells can also secrete growth factors and cytokines into the soluble stromal and neurochemicals into the brain (Li *et al*, 2002; Chen *et al*, 2002*a*, *b*), cross the blood–brain barrier (BBB) and migrate throughout the brain preferentially to areas that have suffered damage (Chen *et al*, 2000; Li *et al*, 2000, 2001; Damme *et al*, 2002). Many previous researchers have reported on mesenchymal stromal cell (MSC) transplantation as a source for autoplastic therapies and improvement in functional recovery after stroke (Chen *et al*, 2000; Li *et al*, 2000, 2001, 2002; Rempe and Kent, 2002; Kurozumi *et al*, 2004).

Hepatocyte growth factor (HGF) is a disulfide-linked heterodimeric protein that was initially purified and cloned as a potent mitogen for hepatocytes and a natural ligand for the c-met proto-oncogene product (Nakamura *et al*, 1984; Matsumoto and Nakamura, 1996). Subsequently, several functions have been ascribed to HGF, including antiapoptosis, angiogenesis, motogenesis, morphogenesis, hematopoiesis, tissue regeneration in a variety of organs, and the enhancement of neurite outgrowth (Matsumoto and Nakamura, 1997; Hayashi *et al*, 2001; Sun *et al*, 2002*a*, *b*; Jin *et al*, 2003). It has also been reported that HGF administration could inhibit the BBB destruction, decrease brain edema, and provide a neuroprotective effect after brain ischemia (Miyazawa *et al*, 1998; Hayashi *et al*, 2001; Shimamura *et al*, 2004).

Recent experimental studies suggest the possibility that gene transduction into MSCs could enhance their existing therapeutic potential (Chen *et al*, 2000; Kurozumi *et al*, 2004). Here, we evaluate the efficiency and effects of gene transduction into MSCs using a replication-incompetent herpes simplex virus type-1 (HSV1764/4-/pR19) vector disabled by the deletion of three critical genes for viral replication encoding infected cell polypeptide (ICP)4, ICP34.5, and virion protein (VP16) (vmw65). This vector contains HSV latency-associated transcript (LAT) promoter and two kinds of enhancer elements: cytomegalovirus (CMV) enhancer and Woodchuck posttranscriptional regulatory elements (WPRE). The availability of this vector has already been examined in the nervous system (Coffin *et al*, 1998; Palmer *et al*, 2000; Lilley *et al*, 2001).

In the present study, we intracerebrally transplanted MSCs in which a gene of interest was transferred with this HSV-1 vector *ex vivo* into a rat transient middle cerebral artery occlusion (MCAO) model under superacute and acute therapeutic time phase, and investigated whether such combined therapy could improve the effects of ischemia.

Materials and methods

Donor Cell Preparation

Marrow stromal cells of adult Wistar rats were prepared following the method described by Azizi *et al* (1998). In brief, the marrow of rat tibias and femurs was extruded with 10 mL of alpha-MEM (Sigma Chemical Co., St Louis, MO, USA) and cultured in the same medium supplemented with 10% fetal bovine serum (FBS), 2 mmol/L L-glutamine, and antibiotic–antimycotic 1 mL/100 mL (GIBCO Invitrogen, Carlsbad, CA, USA) at 37°C, 98% humidity and 5% CO_2. After 48 h, the nonadherent cells were removed by replacing the medium, and the adherent cells were continuously subcultured as MSCs. The fifth to seventh passages were used for the following experiments.

HSV1764/-4/pR19-Hepatocyte Growth Factor Virus and Propagation

One of the authors of the current study (Coffin) constructed the prototype HSV1764/4/pR19GFP virus and has previously described this vector's characteristics (Palmer *et al*, 2000; Lilley *et al*, 2001), which are also described briefly in the Introduction. In the present study, the green fluorescent protein (*GFP*) gene was replaced with a full-length rat HGF complementary DNA (cDNA) tagged with the KT3 (SV (simian virus)40 large, T antigen) epitope (ratHGFKT3) (Sun *et al*, 2002*b*), and the authenticity of this vector (pR19ratHGFKT3WPRE) was confirmed by sequence analysis. Homologous recombination was performed in M49 cells by cotransfection of plasmid pR19ratHGFKT3WPRE DNA and HSV1764/-4/pR19GFP viral DNA. White plaques were selected and purified three times, and replication-incompetent viruses were propagated as described previously (Palmer *et al*, 2000). We ultimately obtained the HSV1764/-4/pR19-HGF virus (HSV-HGF) with a titer of 2×10^8 pfu/mL for use in the present experiments.

Ex Vivo Gene Delivery to MSCs

The cultured MSCs from the fifth to seventh passages were infected with the virus suspension by incubation for 1 h. After infection, the virus suspension was changed to normal culture medium for MSCs and continuously cultured for the subsequent 24 h before transplantation.

Our previous experiments show that the transduction efficiency of the *GFP* gene into the MSCs with our HSV-1 vector is more than 50% even with a multiplicity of infection (MOI) of 5. Here we set the MOI at 5 for the desired gene transfer to MSCs *ex vivo*.

Hepatocyte Growth Factor Detection with Enzyme-Linked Immunosorbent Assay (ELISA) *In Vitro*

We prepared 1.6×10^5 MSCs in each well of a six-well dish. The MSCs were transferred with *HGF* gene by infection with HSV-HGF at MOIs of 0, 0.1, 1, 5, and 10. At 1 h after infection, the infected MSCs were successively incubated with normal culture medium for another 24 h. The culture supernatant and cells were then individually collected through centrifugation. The HGF protein concentrations in MSC culture supernatant and in MSC extracts prepared using 50 mmol/L Tris-HCl (pH 7.4), 150 mmol/L NaCl, 1% Triton X-100, 1 mmol/L phenylmethylsulfonylfluoride (PMSF) (Wako, Osaka, Japan), 2 μg/ml antipain (Peptide Institute Inc., Osaka, Japan), 2 μg/ml leupeptin (Peptide Institute), and 2 μg/ml pepstatin (Peptide Institute) were determined by ELISA using an anti-rat HGF polyclonal antibody (Tokushu Meneki, Tokyo, Japan) as described (Sun *et al*, 2002*b*).

Transient Middle Cerebral Artery Occlusion Animal Model

Experiments were performed on 8-week-old male Wistar rats weighing 250 to 280 g. We induced transient MCAO using the previously described method of intraluminal vascular occlusion (Longa *et al*, 1988). In brief, a length (18.5 to 19.0 mm, determined according to the animal's weight) of 4-0 surgical nylon suture was gently advanced from the external carotid artery into the lumen of the internal carotid artery until it reached the proximal segment of the anterior cerebral artery. After 2 h of MCAO the animals were reanesthetized, and reperfusion was achieved by withdrawing the nylon suture.

The rats were subjected to transient MCAO for 2 h to produce a consistent and reproducible ischemic lesion in the unilateral striatum and cortex.

Intracerebral Transplantation of MSCs

At 2 or 24 h after the onset of MCAO (i.e., on reperfusion), the animals were placed in a stereotactic head holder (model 900, David Kopf Instruments, Tujunga, CA, USA) under inhalation anesthesia. MSCs were intracerebrally transplanted by inserting a 26-gauge needle with a Hamilton syringe into the right striatum (anteroposterior (AP) = 0 mm; lateral to midline (ML) = 2.0 mm; vertical to dura (DV) = 4.5 mm) from bregma, based on the atlas given by Paxinos *et al* (1985). There were 1×10^6 cells in total 10-μl fluid volumes that transplanted into each animal over a 10-min period. No immunosuppressive drugs were used in any animal.

Experimental Groups

In this study, there were seven experimental groups: groups 1 and 5 were treated with phosphate-buffered saline (PBS); groups 2 and 6 were treated with untreated MSCs only; group 3 was treated with the GFP-transferred MSCs (MSC-GFP); and groups 4 and 7 were treated with *HGF* gene-transferred MSCs (MSC-HGF).

Groups 1 to 4 were treated 2 h after MCAO (superacute phase) and groups 5 to 7 were treated 24 h after MCAO (acute phase).

Behavioral Testing

The rats of groups 1 to 4 ($n = 6$) were subjected to a modified neurological severity score (mNSS) test (Schallert *et al*, 1997) to evaluate neurological function before MCAO, at 2 h after MCAO, and at 1, 4, 7, 14, 21, 28, and 35 days after MCAO. The rats of groups 5 to 7 ($n = 6$) were subjected to mNSS before MCAO and at 0, 1, 4, 7, and 14 days after MCAO. These tests are battery of motor, sensory, reflex, and balance tests, which are similar to the contralateral neglect tests in humans. The higher the score, the more severe the neurological deficit (Chen *et al*, 2001).

Infarction Volume

We stained the brains of groups 1, 2, and 4 ($n = 6$) and groups 5 to 7 ($n = 5$) with 2,3,5-triphenyltetrazolium chloride (TTC) (Wako Pure Chemical Industries, Osaka, Japan) to detect the infarction volume of each group at 3 and 14 days after treatment. Briefly, the rats' brains were removed and cut into seven equally spaced (2 mm) coronal sections. These sections were immersed in a 2% solution of TTC at 37°C for 20 mins to reveal the infarcted areas. This procedure is known to reliably mark ischemic damage even at 14 days after MCAO (Bederson *et al*, 1986; Kurozumi *et al*, 2005).

The disposition of the ischemic area was evaluated by calculating the hemispheric lesion area using imaging software (Scion Image, version Beta 4.0.2; Scion Corp., Frederick, MD, USA). To avoid overestimation of the infarct volume, the corrected infarct volume (CIV) was calculated as $CIV = [LT - (RT - RI)] \times d$, where LT is the area of the left hemisphere, RT is the area of the right hemisphere, RI is the infarcted area, and d is the slice thickness (2 mm) (Raymond *et al*, 1990). Relative infarct volumes are expressed as a percentage of contralateral hemispheric volume.

Terminal Deoxynucleotidyltransferase (dUTP) Nick End-Labeling (TUNEL) Staining and Immunohistochemical Assessment

Sample Preparation: At different time points, rats of groups 1, 2, and 4 were reanesthetized and transcardially perfused with saline, followed by 4% paraformaldehyde in PBS. The brain tissues were cut into seven equally spaced coronal blocks. The tissues were processed and 10-μm cryosections were cut.

Immunohistochemical Staining: We can detect three kinds of HGF in this study: the endogenous HGF secreted by the rat ischemic brain tissue after stoke (en-HGF), the exogenous HGF secreted by the transplanted MSCs (ex-HGF-1), and the exogenous HGF delivered from the

HSV-HGF (ex-HGF-2). For the immunohistochemical staining of HGF, the whole rats' brain sections of groups 1, 2, and 4 were prepared on days 2 and 14 after treatment. Rabbit anti-rat HGF primary antibody (prepared by some of the authors of this article, and belonging to the Division of Molecular Regenerative Medicine, Osaka University Graduate School of Medicine, Japan) was used to detect the three kinds of HGF (mixed); a KT3 primary monoclonal antibody (1:1000) (Covance Research Products, Berkeley, CA, USA) was used to detect the ex-HGF-2; a biotinylated universal secondary antibody (VECSTAIN Elite ABC Kit, PK-6200, Vector Laboratories, Burlingame, CA, USA) and a goat anti-rabbit IgG affinity-purified rhodamine-conjugated secondary antibody (1:200) (Chemicon International, Temecula, CA, USA) were also used here. Reaction products were visualized with the VECSTAIN Elite ABC Kit (PK-6200) and a DAB Substrate Kit (Vector Laboratories, Burlingame, CA, USA). To detect the donor MSCs, bisbenzimide (Hoechst 33258; Polysciences, Eppelheim, Germany) was used to fluorescently label cell nuclei *in vitro*. Some sections were counterstained with hematoxylin and observed under a normal light microscope (VB-S20 Multiviewer System, Keyence, Osaka, Japan and Microphot-FXA, Nikon Corp., Tokyo, Japan), and some were directly observed by a fluorescence microscope (BX-50-34-FLAD1, Olympus). The donor MSCs could be detected under ultraviolet (UV) light with blue fluorescence as marked by Hoechst 33258.

To visualize the remaining neurons in the cortex of the ischemic boundary zone (IBZ) of groups 1, 2, and 4 ($n=3$), 7 days after treatment, microtubule-associated protein 2 (MAP-2) was used as the first antibody (1:500) (Chemicon International Inc., CA, USA). Negative control slides for each animal received identical preparation for immunohistochemical staining, except that primary antibodies were omitted.

Terminal Deoxynucleotidyltransferase Nick End-Labeling Staining: At 7 days after treatment, coronal cryosections (10-μm thick) of each rat of groups 1, 2, and 4 ($n=3$) were stained by the TUNEL method for *in situ* apoptosis detection (ApopTag kit, Chemicon International, USA). Specifically, after postfix slides were incubated in a mixture containing terminal deoxynucleotidyl transferase and anti-digoxigenin-rhodamine (Red). Then, they were counterstained with bisbenzimide (Hoechst 33258), which stains blue for each nucleus. The total numbers of TUNEL-positive cells and Hoechst counter-staining positive cells were individually counted in 2 slides from each brain, with each slide containing five random fields from the IBZ, under an × 20 objective of the fluorescence microscope system (BX-50-34-FLAD1, Olympus), using a 3-CCD color video camera (Keyence VB-7010, Keyence, Osaka, Japan).

Statistical Analysis

Data are presented as means ± standard deviations (s.d.). Data from the behavior test (mNSS) were evaluated with repeated-measures analysis of variance (ANOVA), with subsequent Fisher's protected least significant difference (PLSD) test. StatView 5.0 software (SAS Institute, Cary, NC, USA) performing the Student's *t*-test was used to test the CIV data and the difference in means of percentage of the apoptosis-positive cells and the remaining neurons. A difference with a probability value of $P \leq 0.05$ was considered to be statistically significant.

Results

Quantification of Hepatocyte Growth Factor Analysis with Enzyme-Linked Immunosorbent Assay *In Vitro*

As a result, the HGF concentration was approximately 15 times higher in the culture supernatant than in the cell extract at the same MOI, and its increase was correlated with an increase in MOI. Although normal MSCs can produce HGF protein at 0.4 ng/1.6 × 10^5 cells/24 h, after the MSCs were infected with HSV-HGF at an MOI of 5, they were found to produce HGF protein at 2.4 ng/1.6 × 10^5 cells/24 h (Figure 1).

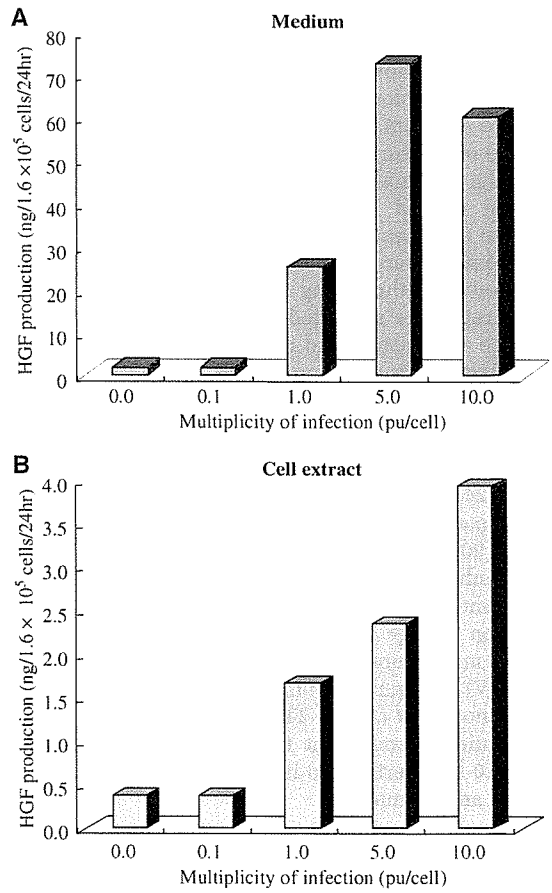

Figure 1 Enzyme-linked immunosorbent assay to determine HGF concentration *in vitro*. Hepatocyte growth factor concentrations were detected in MSC culture supernatant (**A**) and in MSC cell extract. (**B**) After 24 h, 1.6 × 10^5 MSCs were transfected with HSV-HGF at MOIs of 0, 0.1, 1, 5, and 10.

Neurological Outcome

No significant difference in neurological function was detected among all the groups just before cell transplantation. Significant differences of functional recovery were found in group 1 individually compared with group 2 (days 14 to 35, $P<0.05$), with group 3 (days 21 to 35, $P<0.05$), and with group 4 (days 4 and 7, $P<0.05$; days 14 to 35, $P<0.01$) during the observation periods after the superacute transplantation (Figure 2A), and in group 5 individually compared with group 6 (day 14, $P<0.05$), with group 7 (day 7, $P<0.01$ and day 14, $P<0.01$) after the acute transplantation (Figure 2B). Interestingly, we observed significant differences of functional recovery on day 14 among all the superacute treated groups including the MSC-GFP group, which served as a control for *ex vivo* nontherapeutic gene transduction ($P<0.05$). Exceptionally, there was no significant difference only between the MSC-only and the MSC-GFP groups at that time point (Figure 2A). We also found significant neurological recovery on day 14 in the combined therapy group treated even in the acute phase, compared with the MSC-only group treated in the superacute phase (Figure 2C). Also, significant difference of functional recovery on day 14 was found among the groups treated in the acute phase (Figure 2B).

Quantitative Analysis of Infarct Volume

We compared the infarction areas in coronal sections of groups 1, 2, and 4 on day 3 (Figure 3A) and day 14 (Figure 3B), and compared those of groups 5 to 7 on the same time points by TTC staining, and expressed lesion volume as a percentage of contralateral hemispheric volume. At 3 days after treatment, significant difference of %CIV was only detected in the MSC-HGF group compared with the PBS group (34.52% $\pm$3.44% versus 41.83% $\pm$6.25%, $P<0.05$), both of which were treated in the superacute phase (Figure 3C). However, on day 3 there was no significant difference of %CIV among any group that was treated in the acute phase (Figure 3C), while on day 14 there were significant reductions of %CIV in the rats of the MSC-HGF group compared with not only the PBS group but also the MSC-only group treated in the both therapeutic phases (Figure 3D). Also on day 14, the rats treated with MSC-only showed significant reduction in %CIV compared with the PBS group that was treated in the superacute phase (Figure 3D).

Hepatocyte Growth Factor and herpes simplex virus type Gene-Transferred Hepatocyte Growth Factor Detection *In Vivo*

The macrographs presented in Figure 4 showed that mixed HGF protein was diffusely overexpressed in almost the whole ipsilateral brain in the MSC-HGF group compared with other groups, not only on day 2 (column A) but throughout at least the first 2 weeks (column C) after treatment. The microphotographs presented in column B of Figure 4 showed that high HGF expression in the MSC-HGF group could be detected in both the ipsilateral cortex and the ipsilateral basal ganglia at 2 days after treatment. Nevertheless, almost no HGF expression could be detected on the contralateral hemisphere in any treatment group (Figure 4).

Fluorescent staining of groups 1, 2, and 4 on day 14 (Figure 5, column C) also showed higher mixed HGF expression in the MSC-HGF group than that of the other groups. Also, we could detect donor MSCs with blue fluorescence expression by direct observation under UV light (Figure 5, column B). We could identify the HGF expression with red fluorescence in both the transplanted cells and the intercellular space in the transplantation area.

Furthermore, we detected ex-HGF-2 expression, which was transferred from HSV-HGF by anti-KT3 staining (Figures 6D to 6F) of the implantation area. As a result, we had identified ex-HGF-2 expression both in the *HGF* gene-transferred MSCs (arrows in Figure 6G) and in the intercellular space of the transplantation area (arrowheads in Figure 6G) only in the MSC-HGF group (Figure 6F) even 14 days after transplantation. Additionally, we confirmed that MSC itself can also secrete HGF *in vivo* (Figure 6B).

Antiapoptosis

Using TUNEL staining (Figure 7, columns B and C), apoptotic cells with red fluorescence were counted in the IBZ 7 days after treatment, while cells were counted in the same area with blue fluorescence by Hoechst 33258 nuclei marking. In this area we could not detect transferred MSCs; therefore, counterstained cells seemed to be host-derived. The percentage of apoptotic host cells was significantly decreased in the MSC-HGF group (4.92% $\pm$2.15%) compared with the PBS group (22.12% $\pm$4.28%, $P<0.01$) and MSC-only group (10.73% $\pm$5.64%, $P<0.01$). However, there was also significant decrease of apoptotic cells between the MSC-only group (10.73% $\pm$5.64%) and the PBS group (22.12% $\pm$4.28%, $P<0.01$) (Figure 7C).

Neuroprotection

Immunohistochemical staining revealed the remaining neurons of the host with MAP-2 neuronal marker 7 days after treatment (Figure 8A). The percentage of remaining neurons in the cortex of IBZ significantly increased in the MSC-HGF group (20.73% $\pm$2.38%) compared with the PBS group (7.75% $\pm$1.58%, $P<0.01$) and the MSC-only group (12.13% $\pm$3.05%, $P<0.01$). Also, the significant

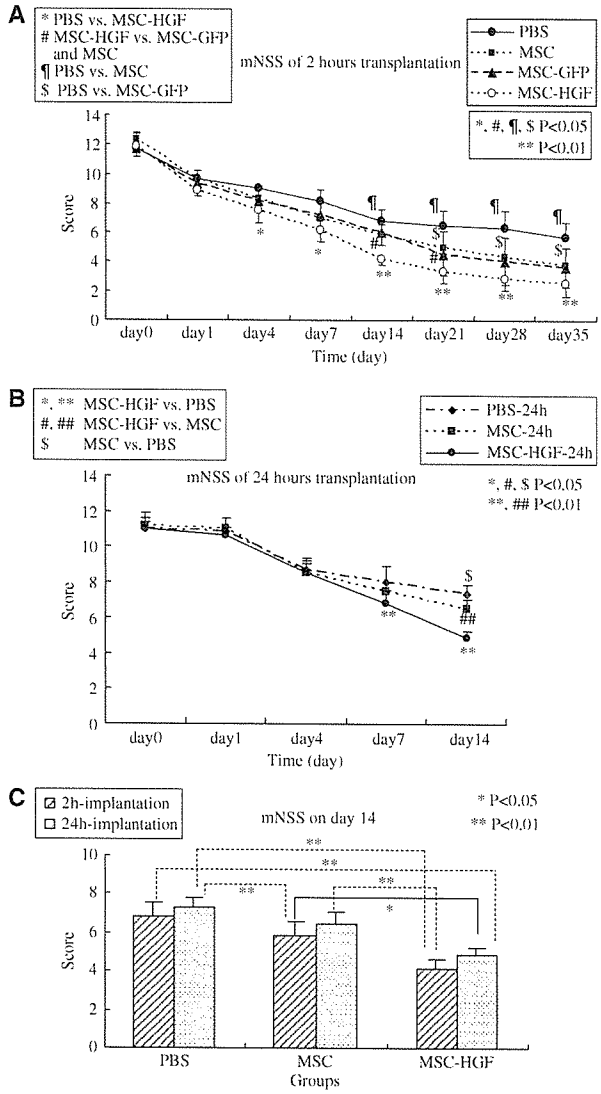

Figure 2 Behavioral functional test (mNSS) before and after MCAO. Groups 1 and 5: treated with PBS; groups 2 and 6: treated with MSC-only; group 3: treated with MSC-GFP; groups 4 and 7: treated with MSC-HGF ($n = 6$ per group). The rats of groups 2 to 7 received 1.0×10^6 cells via intracerebral transplantion in 10 μl PBS. (**A**) Groups 2 to 4 received transplantation 2 h after MCAO (superacute phase); (**B**) groups 4 to 7 received transplantation 24 h after MCAO (acute phase). (**C**) Lists the mNSS on day 14 of groups 1, 2, 4, 5, 6, and 7, showing that the significant neurological recovery among 6 groups while under the comparing condition is only the different therapeutic time phase. Significant functional recovery was detected in the MSC-HGF group compared with the other groups. Data are presented as means $\pm$ s.d.

increase of remaining neurons was found in the MSC-only group (12.13% $\pm$ 3.05%), in comparison with the PBS group (7.75% $\pm$ 1.58%, $P<0.01$) (Figure 8B).

Discussion

Brain ischemia initiates a cascade of events that produces neuronal death and leads to neurological deficits. To prevent brain injury after ischemia, some studies have focused on cell therapies by using embryonic stem cell. But ethical and logistical problems make it unlikely that such therapy could serve as a source of material for therapeutic transplants. Recently, MSC transplantation was reported as a source of autoplastic therapies which not only improve functional recovery after stroke but also have a low risk of tumorigenesis and do not provoke immune reactions (McIntosh and Bartholomew, 2000; Li *et al*, 2002). In the present study, rats of the MSC-only and MSC-HGF groups also showed more significant neurological functional recovery than those of the PBS group.

It is well known that the efficiency of gene transduction to such MSC populations is low, even with virus vectors such as an adenovirus (Ad) (Conget and Minguell, 2000). To date, Kurozumi *et al* (2004) have reported the relatively high efficiency of gene transduction using fiber mutant Ad vector, but the peak level of expression was transient because the Ad vector would not integrate the gene of interest into the genome of the host cells. Lentivirus could express a high efficiency of gene transduction into MSC, but its biosafety remains uncertain because of its origin, the human immunodeficiency virus (Trono, 2000). Retroviruses, which have the ability to integrate the gene of interest into the chromosomes of the host cells, also show a relatively high efficiency of gene transduction to MSC. However, a note of warning was stressed against the potential rise of a neoplasm with a retrovirus-based vector (Pages and Bru, 2004).

In the present study, by the *in vitro* HGF ELISA data and histological detection, we showed that our HSV-1 vector had successfully transferred the gene of interest to the MSC population with high efficiency *in vitro*, and gene-transferred MSCs had successfully functioned *in vivo* to express and maintain a high level of the gene of interest. We confirmed that the increased HGF expression on day 14 was primarily due to the ex-HGF-2 expression that was proven by anti-KT3 staining, as the HSV-1 vector-transferred HGF cDNA was tagged with KT3 epitope. Also, such ex-HGF-2 protein was produced within the *HGF* gene-transferred MSCs and secreted in the intercellular space diffusely in the combined therapy group.

Furthermore, there were no significant differences in functional recovery between the MSC-only group and the MSC-GFP group during the whole detection time course. Also, no obvious difference of apoptosis and the dividing ability was observed between naive MSCs and the *HGF* gene-transferred MSCs in the current study in the first 2 weeks after transplantation (data not shown). It may indicate that gene transfer with HSV-1 vector *ex vivo* would

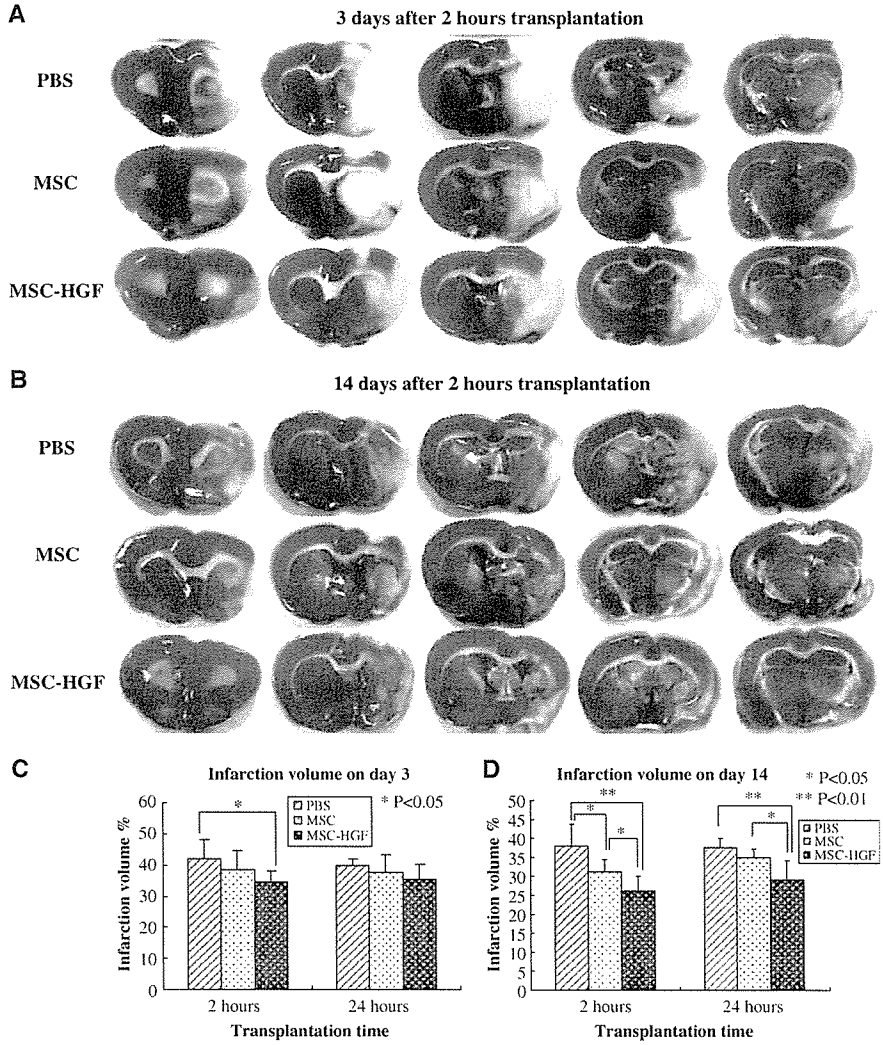

Figure 3 Infarction volume detected by TTC staining. (**A**, **B**) Reduction of infarction areas on days 3 and 14 of groups 1, 2, and 4, which received transplantation 2 h after MCAO occurred: coronal sections stained with TTC. The red region shows intact area; white region shows infarction area. (**C**, **D**) Individually presents the quantification of % CIV in the hemispheric lesion area on days 3 and 14, while being treated at 2 and 24 h after ischemia occurred. Data are presented as means ± s.d. ($P < 0.05$; < 0.01). $n = 6$ for groups 1, 2, 4, and $n = 5$ for groups 5 to 7 at each time point.

not influence the survival and dividing abilities and the therapeutic efficiency of MSCs after transplantation.

So far, to reduce the disability resulting from stroke, some studies have focused on the development of neuroprotective agents such as brain-derived neurotrophic factor, the fibroblast growth factor that effectively prevents delayed neuronal death after transient brain ischemia (Kurozumi *et al*, 2004; Watanabe *et al*, 2004). Recently, overexpression of HGF that can improve the neurological sequalae by neuroprotection, reduce the infarct volume, and the likelihood of brain edema after stroke was reported (Miyazawa *et al*, 1998; Tsuzuki *et al*, 2000; Hayashi *et al*, 2001; Shimamura *et al*, 2004). It suggested that HGF should be one of the most potent growth factors for treating brain ischemia.

To detect the therapeutic efficiency of combined therapy, we tried to treat brain ischemia in the superacute and acute therapeutic phases. Both of them showed significant improvement of neurological deficits compared with MSC-only cell therapy. We got the same result as that Shimamura *et al* (2004) had reported, that HGF had the therapeutic efficiency of reducing the infarction volume after transient MCAO. We also found on day 14 that the MSC-only treated group could significantly reduce the infarction volume under the superacute treatment compared with the PBS-treated group, but not

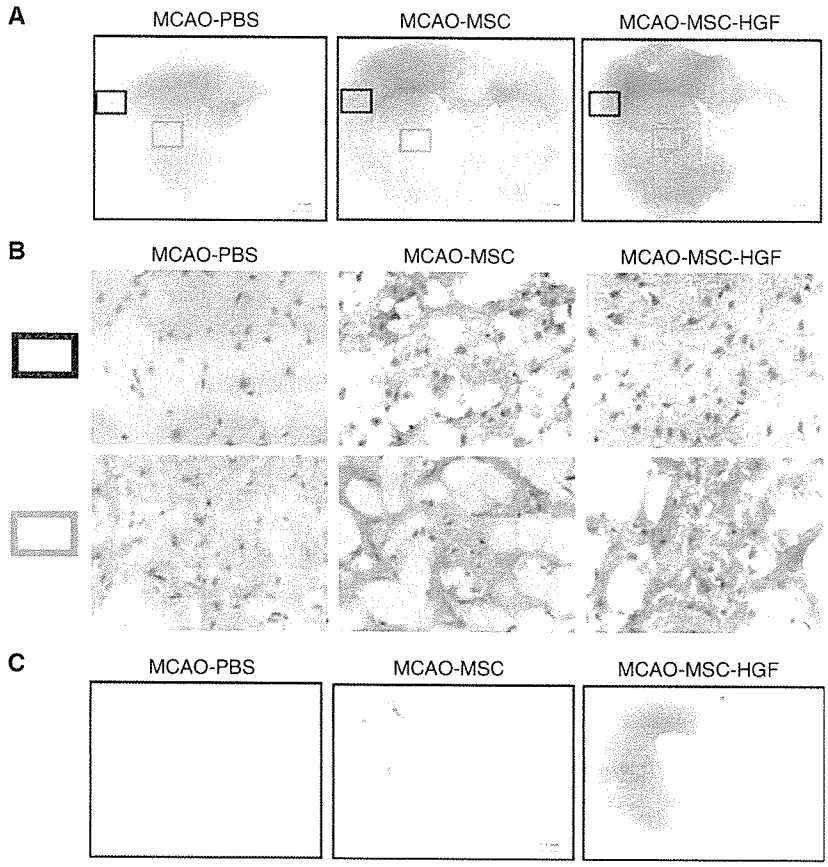

Figure 4 Immunohistochemistry for HGF expression *in vivo*. Mixed HGF expression (brown color) in the ischemic brains of groups 1, 2, and 4 detected by immunohistochemistry on days 2 (row A) and 14 (row C). Scale bar: 1.0 mm. The upper and lower rows identified in B (original magnification, × 400) show the cortex and basal ganglia, respectively, of the images shown in row A.

under the acute treatment. This was the same as the Chopp's group had reported, that transplanted MSCs to the transient MCAO model 24 h after ischemia occurred had improved neurological function recovery, but not significantly decreased infarction area (Chen *et al*, 2000, 2001; Li *et al*, 2000, 2001), while our data of the superacute treatment showed the contrast result. We thought that it might have been caused by the different therapeutic time window. Furthermore, we found significant neurological recovery of the rats treated with combined therapy on day 14, 24 h after MCAO occurred (acuter phase), than the rats of the MSC-only group treated even 2 h after MCAO occurred (superacute phase). It indicates that our combined therapeutic method may extend the therapeutic time window for treating brain ischemia at least until 24 h after the onset of MCAO, while compared with the MSC-only cell therapy. To treat transient ischemia, both the combined therapeutic method and superacute therapeutic time window might be important.

Mesenchymal stromal cell-only therapy also showed significant improvement of functional outcome and decrease of infarction volume when cells were administered 2 h after stroke. A more likely mediator of short-term benefit may reflect increased production of growth factors, including neurotrophins adjusted to the needs of the compromised tissue with an array of reducing host cells' apoptosis in the IBZ, including neurons, and promoting functional recovery of the remaining neurons (David and Thomas, 2002; Chopp and Li, 2002). After stroke, cerebral tissue reverts to an earlier stage of development and thus becomes highly responsive to stimulation by cytokines, trophins, and growth factors from the invading MSCs (Chopp and Li, 2002). The MSCs may simply provide the resources required by the ontogenous cerebral tissue to stimulate cerebral remodeling.

In the present study, the combined therapy group showed more therapeutic benefit than the MSC-only cell therapy. Hepatocyte growth factor gene-modified MSCs may also behave as small molecular factories, secrete an array of cytokines and trophic factors over an extended period and not in a single bolus dose, directly involved in promoting plasticity of the ischemic damaged neurons or in stimulating

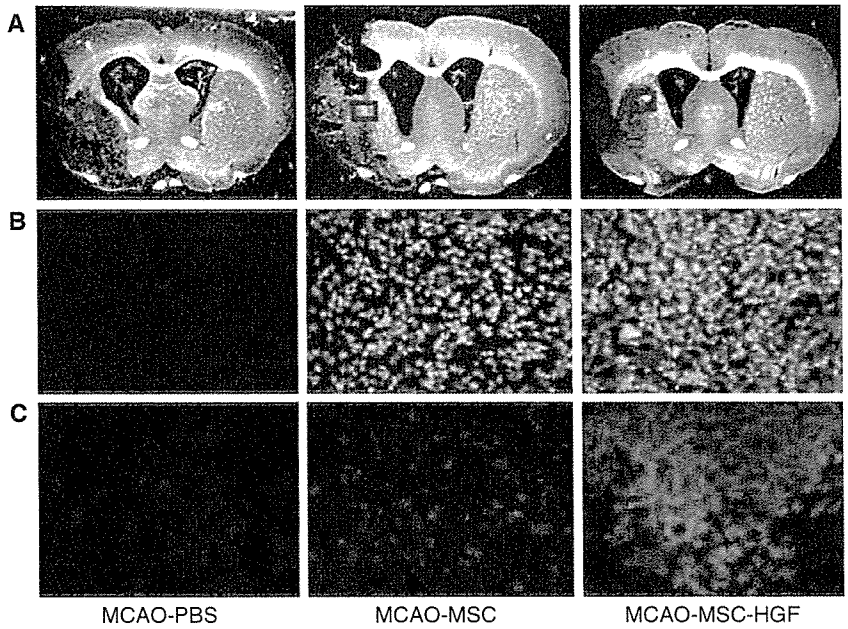

Figure 5 Expression of HGF and identification of transplanted MSCs. Photographs in row C show mixed HGF expression in the ipsilateral brain of groups 1, 2, and 4 with red fluorescence, and photographs in row B show transplanted donor MSCs of groups 2 and 4 with blue fluorescence, at 2 weeks after treatment. The microphotographs shown in rows B and C have the same size and higher power magnification than the blue squares in row A. Original magnification, × 200.

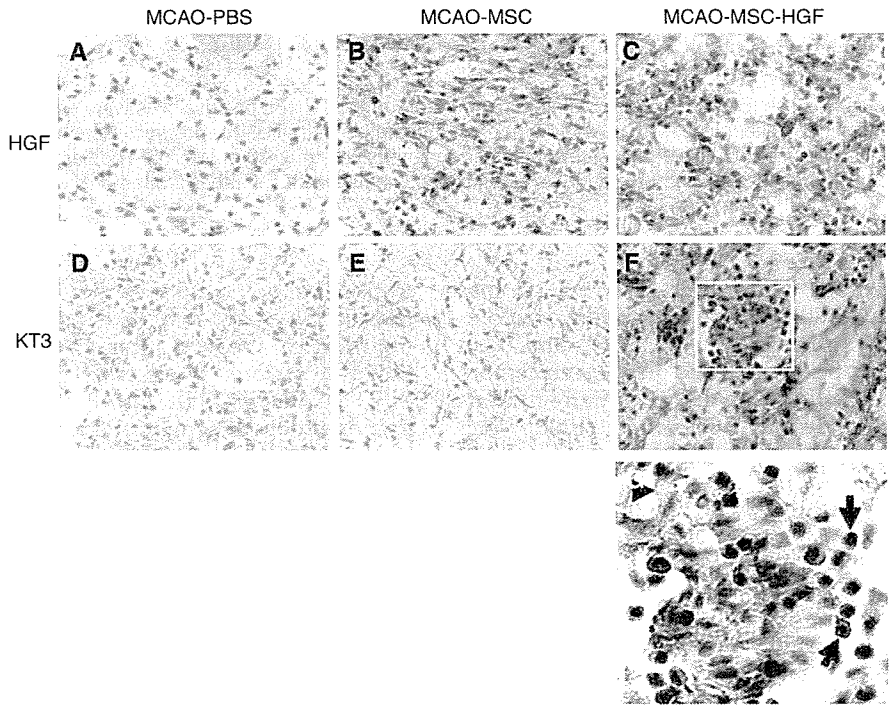

Figure 6 Immunohistochemistry for HSV-1 vector-transferred exogenous HGF and mixed HGF expression. The upper column (**A–C**) shows mixed HGF expression in groups 1, 2, and 4 with anti-rat HGF immunostaining, and the lower column (**D–F**) shows ex-HGF-2 expression with anti-ratHGFKT3 immunostaining at 2 weeks after treatment. Original magnification, × 200. (**G**) is the enlarged white square in (**F**), arrows mark HGF expression in the transplanted MSCs and an arrowhead marks HGF expression in the intracellular space.

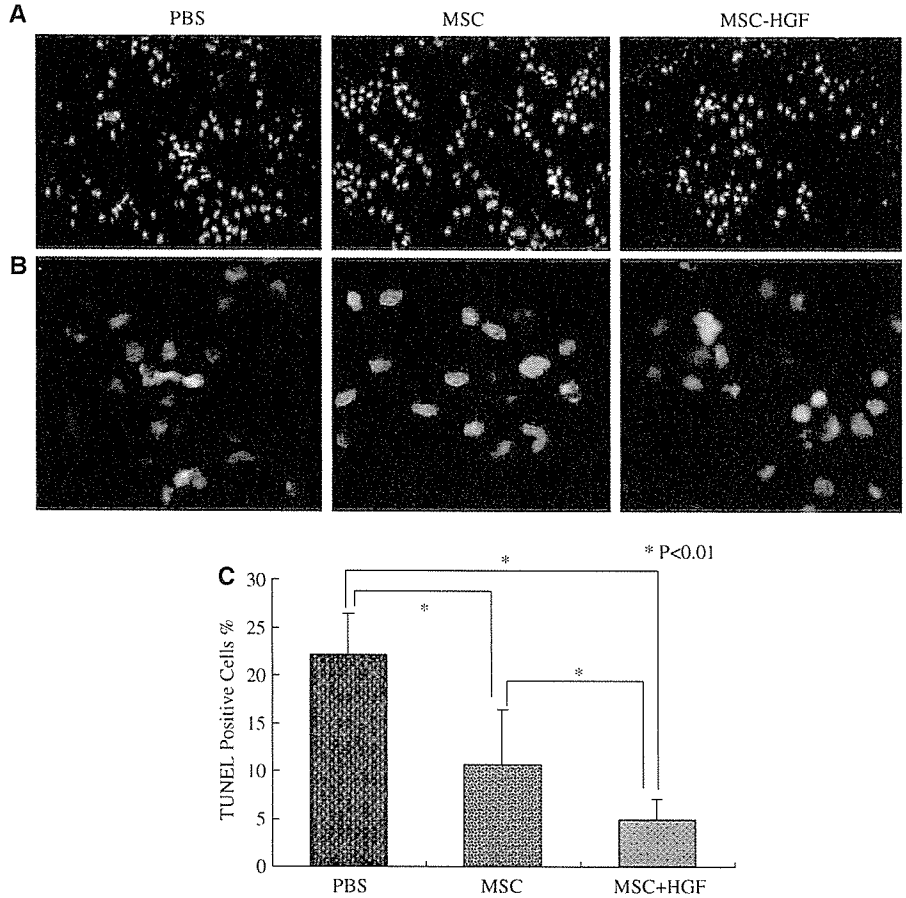

Figure 7 Apoptotic cells in the IBZ with TUNEL staining. (**A**) Column, fewer TUNEL-positive cells were detected in rats treated with MSC-HGF than others treated either with PBS or MSC-only (Rhodamine, red, TUNEL positive; Hoechst, blue, nuclear; original magnification with × 40 object). (**B**) Column, 4 times enlarged magnification of × 40 object. (**C**) The percentage of TUNEL-positive cells in the IBZ was significantly reduced in the MSC-HGF group compared with the other groups 7 days after treatment.

glial cells to secrete neurophins. Marrow stromal cells secrete many cytokines known to play a role in hematopoiesis (Dormady *et al*, 2001), and also supply autocrine, paracrine, and juxtacrine factors that influence the cells of the marrow microenvironment themselves (Haynesworth *et al*, 1996). The interaction of MSCs with the host brain may lead MSCs and parenchymal cells also to produce abundant trophic factors, which may contribute to recovery of function lost as a result of a lesion too (Williams *et al*, 1986).We speculate that *HGF* gene-modified MSCs also had carried out such ways not only to produce extended and abundant exogenous HGF, but also a variety of other cytokines and trophic factors, and interact with each other in an anatomically distributed, tissue-sensitive, and temporally ongoing way.

Other functions of HGF include reducing the BBB destruction without exacerbating cerebral edema, decreasing intracranial pressure, inducing angiogenesis, and interacting with other kinds of neurotrophic factors; cytokines that are secreted by MSCs themselves may also take part in improving the neurological recovery after stroke. We also speculate that the various cytokines secreted from MSCs or MSC-HGF activate the proliferation and differentiation of endogenous neural stem and progenitor cells in the subventricular zone, such as Chopp and Li (2002) had reported. Also, transplanted MSCs themselves might differentiate into some kinds of central never system cells (Woodbury *et al*, 2000). Actually, we also found some MSCs expressing glial phenotype 4 weeks after transplantation only in the combined therapy group (data not shown), which might suggest that *HGF* gene transduction could influence transplanted MSC differentiation. But tissue regeneration might be another part of the mechanisms that induced recovery after stroke mainly occurs in the chronic therapeutic time course.

Anyhow, our MSC-HGF combined therapy enhanced the therapeutic efficiency than the MSC-only

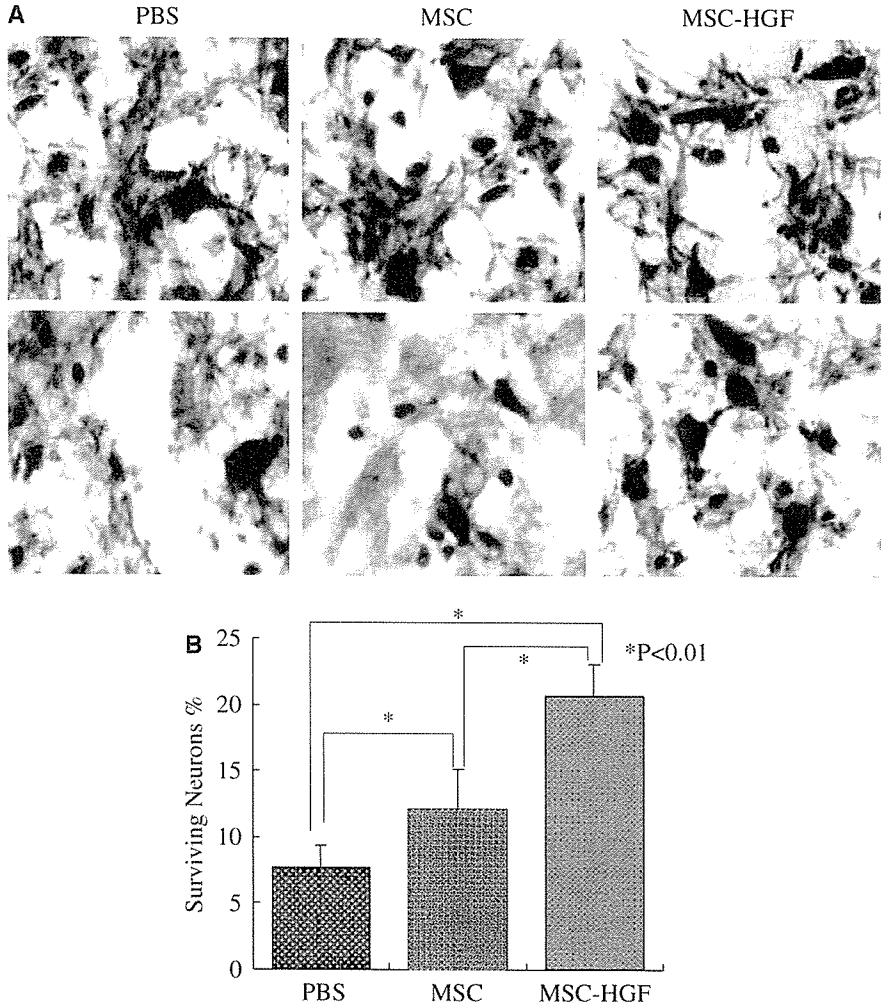

Figure 8 Remaining neurons in the cortex of IBZ with MAP-2 immunostaining. (**A**) Column, more neurons could be detected in rats treated with MSC-HGF than others treated either with PBS or MSC-only (MAP-2, dark brown, neurons; hematoxylin, blue, nuclear; original magnification, × 600). (**B**) The percentage of neurons in the cortex of IBZ was significantly increased in the MSC-HGF group compared with the other groups 7 days after treatment.

cell therapy for stroke in rats treated in both the superacute and acute phases. The target gene was successfully transferred to MSCs with the HSV-1 virus vector *in vitro*, and later the gene-modified MSCs served as both a therapeutic material and a vector platform that continuously carried the target gene into the brain and functioned *in vivo*. This method might be safer than direct gene transfer with viral vectors for *in vivo* treatments, more therapeutically efficient than MSC-only cell therapy, extend the therapeutic time window from superacute to at least 24 h after ischemia happened, and also could be used as a post-treatment method for stroke. Although the best therapeutic time schedule, the administration route of MSCs and best cytokine gene (or cocktail of the genes) should be explored for better clinical application. It may require a broad array of treatments to prevent neurological disorders in brain ischemia, which may offer a promise for human clinical treatment in future.

References

Azizi SA, Stokes D, Augelli BJ, DiGirolamo C, Prockop DJ (1998) Engraftment and migration of human bone marrow stromal cells implanted in the brains of albino rats—similarities to astrocyte grafts. *Proc Natl Acad Sci USA* 95:3908–13

Bederson JB, Pitts LH, Germano SM, Nishimura MC, Davis RL, Bartkowski HM (1986) Evaluation of 2,3,5-triphenyltetrazolium chloride as a stain for detection and quantification of experimental cerebral infarction in rats. *Stroke* 17:1304–8

Caplan AI, Bruder SP (2001) Mesenchymal stem cells: building blocks for molecular medicine in the 21st century. *Trends Mol Med* 7:259–64